Brain Pathology ISSN 1015-6305

RESEARCH ARTICLE

Vascular Endothelial Growth Factor and Nitric Oxide Production in Response to Hypoxia in the Choroid Plexus in Neonatal Brain

Viswanathan Sivakumar, MBBS, PhD[1]; Jia Lu, PhD[2]; Eng Ang Ling, PhD[1]; Charanjit Kaur, PhD[1]

[1] Department of Anatomy, Yong Loo Lin School of Medicine, National University of Singapore, Singapore.
[2] Defence Medical and Environmental Research Institute, Singapore.

Corresponding author:
C. Kaur, Department of Anatomy, Yong Loo Lin School of Medicine, Blk MD10, 4 Medical Drive, National University of Singapore, Singapore 117597 (E-mail: *antkaurc@nus.edu.sg*)

doi:10.1111/j.1750-3639.2007.00104.x

Abstract

Damage to the choroid plexus in 1-day-old Wistar rats subjected to hypoxia was investigated. The mRNA and protein expression of hypoxia-inducible factor-1α (HIF-1α), endothelial, neuronal, inducible nitric oxide synthase (eNOS, nNOS, iNOS), and vascular endothelial growth factor (VEGF) along with nitric oxide (NO) production and VEGF concentration was up-regulated significantly in hypoxic rats. Ultrastructurally, the choroid plexus epithelial cells showed massive accumulation of glycogen. A striking feature was the extrusion of cytoplasmic fragments from the apical cell surfaces into the ventricular lumen following the hypoxic insult. Intraventricular macrophages showed increased expression of complement type 3 receptors, major histocompatibility complex class I and II antigens, and ED1 antigens. Following an intravenous injection of horseradish peroxidase (HRP), a large number of intraventricular macrophages were labeled suggesting enhanced leakage of the tracer from the blood vessels in the choroid plexus connective tissue stroma into the ventricular lumen. We suggest that increased production of NO in hypoxia is linked to the structural alteration of the choroid plexus, and along with VEGF, may lead to increased vascular permeability. Melatonin treatment reduced VEGF and NO levels as well as leakage of HRP suggesting its potential value in ameliorating damage in choroid plexus pathologies.

INTRODUCTION

The choroid plexus synthesizes and secretes cerebrospinal fluid (CSF) and plays an important role in supporting neuronal metabolism (56). It establishes and maintains the extracellular milieu throughout the brain, in part by secreting numerous growth factors into the CSF (8) which has an important role in the development of the nervous system (38, 46). Investigation of CSF composition plays a significant role in diagnosis and management of many neurological diseases (60).

Hypoxia/ischemia in the perinatal period is associated with subependymal and intraventricular hemorrhages (28) as well as ventricular enlargement (43) leading to a poor neurodevelopment outcome (61). The choroid plexus, ependyma and the subventricular zone in the developing brain are extremely vulnerable in hypoxic/ischemic conditions (50). Although occurrence of intraventricular hemorrhages and damage to the choroid plexus have been reported in hypoxic/ischemic conditions, the factors that might be responsible for this damage remain to be clarified. Among several putative factors, nitric oxide (NO) has been considered as a major one associated with perinatal hypoxia/ischemia-induced neurological abnormalities (6, 22). Indeed, increased NO levels have been reported in the CSF and brain parenchyma of newborn infants in hypoxic/ischemic conditions (9, 22). However, it remains to be elucidated if NO is responsible for causing damage to the choroid plexus in hypoxic conditions. This notion takes into consideration the fact that neuronal nitric oxide synthase (nNOS) expression has been reported in the choroid plexus (30) and that NO has been demonstrated to play a role in choroidal blood flow (57). Furthermore, NO derived from the inducible nitric oxide synthase (iNOS) has inflammatory properties and is implicated in secondary brain damage (48, 22).

Hypoxia-inducible factor-1α (HIF-1α) is a transcription factor expressed uniquely in response to physiologically relevant levels of hypoxia (52). It plays a central role in transcription of hypoxia-responsive genes such as vascular endothelial growth factor (VEGF) (53) which increases the permeability of the blood vessels (39, 51, 62). Hypoxia has also been reported to induce iNOS mRNA transcription and expression (42) and up-regulate nNOS expression (3). Up-regulation of endothelial nitric oxide synthase (eNOS) in hypoxic/ischemic conditions has been described to induce vasodilation to increase blood flow (4).

In light of the above, we aimed to investigate the mRNA and protein expression of HIF-1α, VEGF, eNOS, nNOS, and iNOS in the choroid plexus of neonatal rats following a hypoxic exposure. VEGF concentration and the amount of NO produced in response

Table 1. Number of rats sacrificed at various time points after the hypoxic exposure (in brackets) and their age-matched controls for various methods. Abbreviations: RT-PCR = reverse transcription polymerase chain reaction; EIA = enzyme immunoassay; NO = nitric oxide.

Control (hypoxic)	Immunohistochemistry	RT-PCR	Western blotting EIA and NO assay	Electron microscopy
1 day (3 h)	3 (3)	5 (5)	5 (5)	3 (3)
2 days (24 h)	3 (3)	5 (5)	5 (5)	3 (3)
4 days (3 days)	3 (3)	5 (5)	5 (5)	3 (3)
8 days (7 days)	3 (3)	5 (5)	5 (5)	3 (3)
15 days (14 days)	3 (3)	5 (5)	5 (5)	3 (3)

Six rats not shown in the table were used for periodic acid Schiff staining (three control and three at 3 h after hypoxic exposure). Another 14 rats were given melatonin.

to hypoxia were also measured. As hypoxia is known to alter the glycogen concentration in many tissues (40), we determined its content in the choroid plexus by periodic acid Schiff (PAS) staining. The permeability of the blood vessels was assessed by an intravenous injection of horseradish peroxidase (HRP) and its passage through the choroid plexus was then followed.

In addition to the above, the immunophenotypic profiles of intraventricular macrophages were also examined for possible signs of activation following the hypoxic exposure. It is known that the intraventricular macrophages express complement type 3 receptors (CR3), major histocompatibility complex class I (MHC I) and class II (MHC II) antigens, and macrophage/monocyte antigens (23). Hence, changes in the expression of above receptors/antigens in response to hypoxia were examined.

Although previous studies have shown damage to the choroid plexus in 7-day-old rats at 4 h following ligation of the common carotid artery and exposure to hypoxia (50), the changes in expression of HIF-1α, VEGF, eNOS, nNOS, and iNOS have not been reported. In view of this, we aimed to examine the ultrastructure of the choroid plexus epithelial cells and their associated macrophages for any alteration following hypoxic exposure at birth up to 14 days after the hypoxic exposure and correlate them with the changes in production of VEGF and NO.

METHODS

Animals

One hundred and one 1-day-old Wistar rats were exposed to hypoxia in a decompression chamber (Model 16M, ETC, Southampton, PA, USA) for 2 h at an atmospheric pressure of 350 mmHg (pO2 73 mm Hg). They were then allowed to recover under normobaric conditions for 3, 24 h, 3, 7, or 14 days before sacrifice. Another group of 87 rats were used as age-matched controls. These were kept outside the chamber (atmospheric pressure 760 mm Hg, pO2 159 mm Hg).

The number of hypoxic rats and their age-matched controls used for each of the methods described below is shown in Table 1. In the handling and care of animals, the International Guiding Principles for Research [WHO Chronicle 39 (2): 51–56 (1985)] and as adopted by the Laboratory Animals Centre, Animal Holding Unit, National University of Singapore were followed.

Melatonin administration

To assess the effect of melatonin on VEGF concentration, NO production, and vascular permeability in the choroid plexus, 14 rats were given intraperitoneal injections of melatonin dissolved in normal saline (10 mg/kg body weight) as described by us previously (24). Each rat received the first injection of melatonin immediately before exposure to hypoxia, the second injection immediately after exposure to hypoxia, and a third injection at 1 h after exposure to hypoxia. VEGF concentration and NO production in the choroid plexus were determined at 3 and 24 h (n = 5 rats at each time interval). The values between the hypoxic and hypoxic + melatonin-administered rats were compared statistically.

Hypoxic rats treated with melatonin as mentioned above were also used for tracer studies as described below.

Real-time reverse transcription polymerase chain reaction (Real-time RT-PCR)

Choroid plexus in the lateral ventricles was dissected and removed from the hypoxic rats and their corresponding controls, immediately frozen in liquid nitrogen and stored at −80°C until RNA isolation. Total RNA was extracted from the tissue using RNAesy mini kit (Qiagen, Valencia, CA, USA) according to the manufacturer's protocol. The amount of total RNA was quantified with a Biophotometer (Eppendorf AG, Hamburg, Germany). The reverse transcription was performed as described previously (25).

Quantitative RT-PCR

Quantitative RT-PCR was carried out on a Lightcycler 3 instrument using a FastStart DNA Master plus SYBR Green I kit (Roche Diagnostics GmbH, Roche Applied Science, Mannheim, Germany) according to the manufacturer's instructions. Briefly, a Lightcycler master mix was prepared using 2 µL of Lightcycler-FastStart DNA Master plus SYBR Green I with forward and reverse primers at a final concentration of 0.5 µM each. Two microlitres of the cDNA was added into 18 µL of Lightcycler master mix and transferred into Lightcycler glass capillaries. The capillaries were capped, placed in a Lightcycler carousel and centrifuged in a specific Lightcycler centrifuge. Thermal cycling was carried out. The first segment of the amplification cycle consisted of a denaturation program at 95°C for 10 minutes. The second segment consisted of denaturation, primer annealing, elongation, and quantification program repeated for 40 cycles. The third segment consisted of a melting curve program. The final segment consisted of a cooling program at 40°C.

The amplified PCR products were separated on a 1.5% agarose gel staining with eithidium bromide and photographed (Chemi

Table 2. Sequence of specific primers. Abbreviations: HIF-1α = hypoxia-inducible factor-1α; VEGF = vascular endothelial growth factor; eNOS = endothelial nitric oxide synthase; iNOS = inducible nitric oxide synthase; nNOS = neuronal nitric oxide synthase.

Primer	Forward	Reverse	Amplicon size (bp)
HIF-1α	tcaagtcagcaacgtggaag	tatcgaggctgtgtcgactg	198
VEGF	agaaagcccaatgaagtggtg	actccagggcttcatcattg	177
eNOS	tggcagccctaagacctatg	agtccgaaaatgtcctcgtg	243
iNOS	ccttgttcagctacgccttc	ggtatgcccgagttctttca	179
nNOS	ccggaattcgaataccagcctgatc	ccgaattcctccaggagggtgtccaccgcatg	617
β-Actin	tcatgaagtgtgacgttgacatccgt	cctagaagcatttgcggtgcaggatg	285

Genius[2] image analyzer, Cambridge, UK). Expressions of target genes were measured in triplicate and were normalized to β-actin, as an internal control. Forward and reverse primer sequence for each gene and their corresponding amplicon size are provided in Table 2. Gene expression was quantified using a modification of the $2^{-\Delta\Delta ct}$ method as previously described (33).

Western blotting

Choroid plexus was removed from the lateral ventricles from the hypoxic rats and their corresponding controls and was snap-frozen in liquid nitrogen and stored at −80°C. The tissues were homogenized with tissue protein extraction reagent (Pierce Biotechnology, Rockford, IL, USA) containing protease inhibitors. All procedures were carried out at 4°C. Homogenates were centrifuged at 15 000 *g* for 10 minutes and the supernatant was collected. Protein concentrations were determined by using bovine serum albumin (Sigma-Aldrich, MI, USA) as a standard. Samples of supernatants containing 20 μg of protein were heated to 95°C for 5 minutes and protein was separated by sodium dodecyl sulphate-polyacrylamide gel electrophoresis (SDS-PAGE) in 12% gels, in a Mini-Protein II apparatus (Bio-Rad Laboratories Inc, Hercules, CA, USA). Protein bands were electroblotted onto 0.45 μm polyvinylindene difluoride (PVDF) membranes (Bio-Rad) at 1.5 mA/cm^2 of membrane for 1 h in Towbin buffer, pH 8.3, to which 20% (v/v) methanol had been added. After transfer, the membranes were blocked with 5% (w/v) non-fat dried milk and 0.05% (v/v) Tween-20 in 20 mM Tris-HCl buffer, pH 7.6, containing 137 mM sodium chloride (TBST). The membranes were then separately incubated with dilutions of the polyclonal VEGF (1:1000), nNOS (1:500), and monoclonal HIF-1α (1:500), eNOS (1:2500), and iNOS (1:3000) antibodies in blocking solution overnight at 4°C. They were then incubated with the secondary antibodies, HRP-conjugated anti-rabbit, 1:5000 for VEGF and nNOS and HRP-conjugated anti-mouse, 1:5000 (GE Healthcare, Amersham, UK) for HIF-1α, eNOS, and iNOS. Specific binding was revealed by an enhanced chemiluminescence kit (GE Healthcare) following the manufacturer's instructions. For load control, after intensive washing, membranes were incubated with monoclonal mouse anti-actin (1:3000) (Sigma-Aldrich). Precision pre-stained standards (Bio-Rad) were used as molecular weight markers. X-ray films (GE Healthcare) were scanned with a computer-assisted G-710 densitometer (Bio-Rad) to quantify band optical density using Quantity One software (Bio-Rad).

Analysis of VEGF by enzyme immunoassay (EIA)

The amount of VEGF released in the choroid plexus samples from control, hypoxic, and hypoxia + melatonin rats was determined using *Chemikine*™ VEGF EIA kit (Chemicon International Inc, Temecula, CA, USA). Choroid plexus was homogenized in tissue protein-extracting reagent buffer (Pierce Biotechnology). EIA measurements were performed according to the manufacturer's protocol. The optical density was measured at 490 nm. The amount of VEGF detected in each sample was compared with a VEGF standard curve.

Nitrite assay

The total amount of NO in the choroid plexus samples from control, hypoxic, and hypoxia + melatonin rats was assessed by the Griess reaction, using a colorimetric assay kit (US Biological, Swampscott, MA, USA) that detects nitrite (NO_2^-), a stable reaction product of NO. Homogenates as described above for VEGF EIA were prepared and nitrite concentration was quantified according to manufacturer's instructions. The optical density of the samples was measured at 540 nm using with GENios microplate reader (TECAN Austria GmbH, Salzburg, Austria). The nitrite concentration was determined from a nitrite standard curve.

Statistics

For RT-PCR, Western blots, EIA, and nitrite assay, data are reported as mean ± SD. A Student's *t*-test was used to determine the statistical significance of differences in values between normal and hypoxic or between hypoxic and hypoxia + melatonin rats. A value of $P < 0.05$ was considered significant.

Immunohistochemistry

Rats exposed to hypoxia and their corresponding controls were anesthetized with 6% sodium pentobarbital and perfused with an aldehyde fixative composed of a mixture of periodate-lysine-paraformaldeyde with a concentration of 2% paraformaldehyde. The brains were removed and frozen coronal sections at 40 μm thickness containing the lateral ventricles were cut with a Frigocut cryotome (Leica Instruments GmbH, NuBloch, Germany). They were incubated with VEGF, nNOS, eNOS, iNOS, OX-42, ED1, OX-18, and OX-6 antibodies at dilutions shown in Table 3, in

Antibody	Host	Source	Dilution
VEGF	Rabbit—polyclonal	Santacruz Biotechnology, Inc., Santacruz, CA, USA	1:200
eNOS	Mouse—monoclonal	BD Transduction Laboratories, San Jose, CA, USA	1:250
iNOS	Mouse—monoclonal	BD Transduction	1:1000
nNOS	Rabbit—polyclonal	BD Transduction	1:500
OX-42	Rat—monoclonal	Harlan-Sera-Lab Ltd, Loughborough, UK	1:100
OX-18	Rat—monoclonal	Haralan-Sera-Lab	1:100
OX-6	Rat—monoclonal	Haralan-Sera-Lab	1:100
ED1	Rat—monoclonal	Serotec, Oxford, UK	1:400

Table 3. Antibodies used for immunohistochemistry. Abbreviations: VEGF = vascular endothelial growth factor; eNOS = endothelial nitric oxide synthase; iNOS = inducible nitric oxide synthase; nNOS = neuronal nitric oxide synthase.

phosphate-buffered saline (PBS), respectively, for 16–20 h. OX-42, OX-18, and OX-6 antibodies detect CR3 receptors, MHC I and MHC II antigens respectively on the microglial cells. ED1 recognizes cells of monocyte/macrophage lineage. Subsequent antibody detection was carried out by using Vectastain ABC kit (PK4001 and 4002, Vector Laboratories, St. Louis, MI, USA) against rabbit and mouse immunoglobulin G with 3, 3′-diaminobenzidine tetrachloride (DAB) as a peroxidase substrate. For negative controls, some sections from each group were incubated in a medium omitting the primary antibodies.

PAS staining

Rats at 3 h after exposure to hypoxia and their corresponding controls were anesthetized and perfused with an aldehyde fixative as described above for immunohistochemistry. The brains were removed and kept in a similar fixative as above for 4 h following which they were kept at 4°C overnight in 0.1 M phosphate buffer containing 15% sucrose. Frozen coronal sections of the brain were cut at 40 μm thickness and were incubated for 5 minutes in 0.5% periodic acid, and then Schiff's reagent at room temperature. After several washes with tap and deionized water the sections were counterstained by Shandon hematoxylin nuclear stain for 10 s, dehydrated by immersion in alcohol, and then cleared with histoclear before mounting in Permount medium.

Electron microscopy

The hypoxic rats and their corresponding controls were anesthetized with 6% sodium pentobarbital and were perfused with a mixed aldehyde fixative composed of 2% paraformaldehyde and 3% glutaraldehyde in 0.1 M phosphate buffer, pH 7.3. After perfusion, the brains were removed and coronal slices (approximately 1 mm thickness) containing the lateral ventricles were cut at the level of optic chiasma. Vibratome sections of 80–100 μm thickness were cut out from these blocks and rinsed overnight in 0.1 M phosphate buffer. They were then post-fixed for 2 h in 1% osmium tetraoxide, dehydrated and embedded in Araldite mixture. Ultrathin sections were cut and viewed in a Philips CM 120 electron microscope.

Tracer studies

Control, hypoxic, and hypoxia + melatonin rats (n = 4; 24 h after the hypoxic exposure) were given an intravenous injection of HRP (type VI, Sigma Aldrich, St. Louis, MI, USA) via the left external jugular vein (0.5 μL/g body weight; 7.2 mg of HRP dissolved in 50 μl of saline). Our earlier study had shown that HRP is extravasated from the blood vessels to the CSF after 30 minutes to 1 h (35) following intravenous administration. On this basis, the rats in the present study were sacrificed by perfusion at 3 h after the HRP injection using a fixative composed of 1.25% glutaraldehyde and 1% paraformaldehyde. The choroid plexus was removed and processed for light microscopy as previously described (35).

RESULTS

Analysis of HIF-1α, VEGF, eNOS, nNOS, iNOS mRNA expression (Figure 1)

At 3 and 24 h after hypoxia, the expression of HIF-1α mRNA in the choroid plexus was increased significantly ($P < 0.05$) in comparison with the controls; thereafter, the expression level was decreased drastically. VEGF mRNA was progressively increased significantly at 3 h to 14 days in comparison with the control values ($P < 0.05$). Increase in eNOS mRNA was most marked at 3, 24 h and 3 days followed by a decrease at 7 and 14 days. Expression of iNOS mRNA showed a significant increase at 3, 24 h, 3, and 7 days in hypoxic rats. At 14 days, however, it was significantly reduced. nNOS mRNA was elevated up to 3 days when compared with the controls ($P < 0.05$) but it showed a significant decrease at 7 and 14 days.

Figure 1. Reverse transcription polymerase chain reaction (RT-PCR) analysis of hypoxia-inducible factor-1α (HIF-1α), vascular endothelial growth factor (VEGF), endothelial, inducible, and neuronal nitric oxide synthase (eNOS, iNOS, and nNOS) gene expression in the choroid plexus of rats subjected to hypoxia at postnatal day 1. Left panel represents 1.5% agarose gel stained with ethidium bromide of RT-PCR products of the above-mentioned mRNA in the choroid plexus of rats at 3, 24 h, 3, 7, and 14 days after the hypoxic exposure and their corresponding controls (C). Right panel shows the graphical representation of fold changes quantified by normalization to the β-actin as an internal control. Each bar represents the mean ± SD. Differences in the mRNA levels are significant (*$P < 0.05$) after the hypoxic exposure when compared with controls.

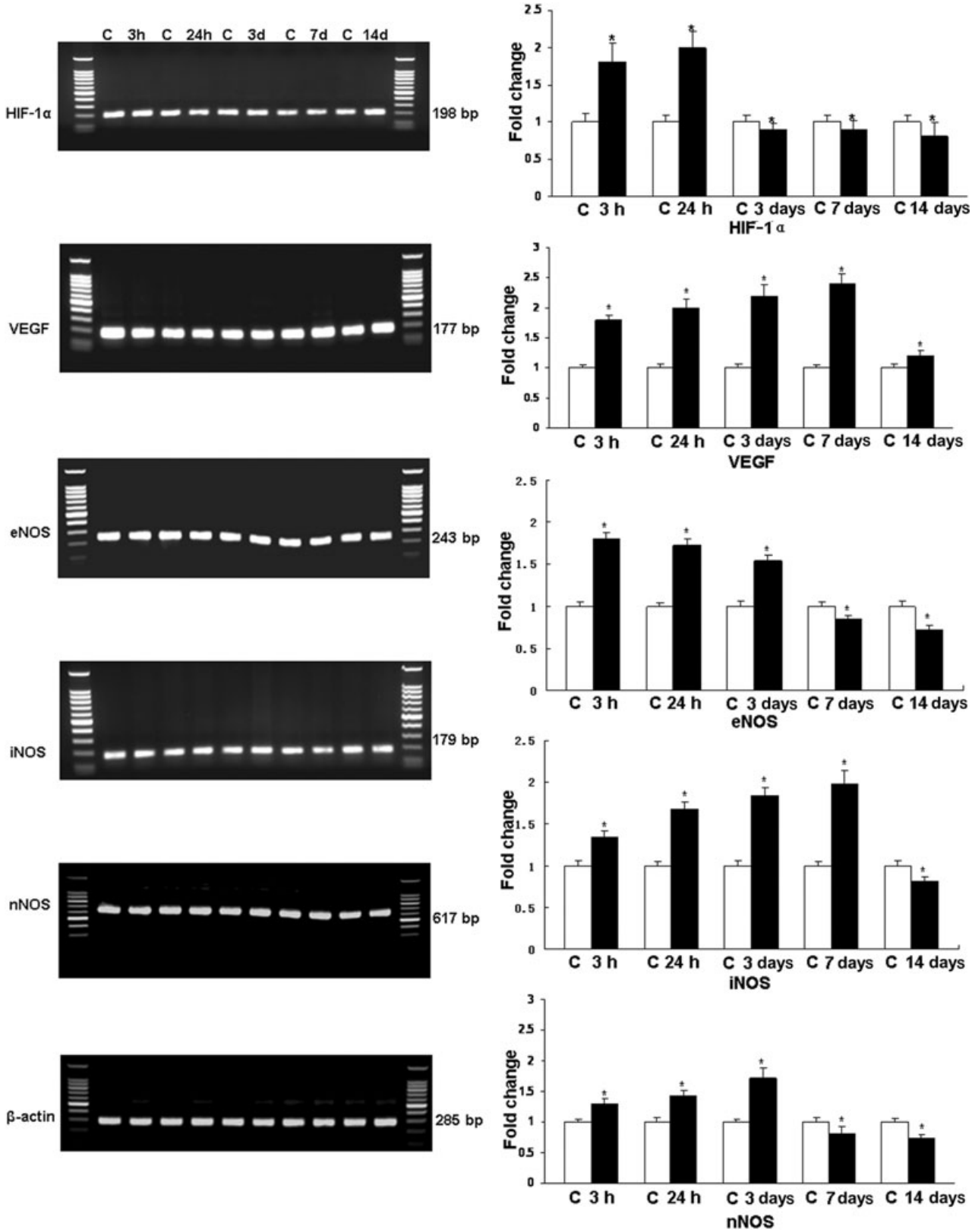

Figure 2. Western blotting of hypoxia-inducible factor-1α (HIF-1α), vascular endothelial growth factor (VEGF), endothelial, inducible, and neuronal nitric oxide synthase (eNOS, iNOS, and nNOS) protein expression in the choroid plexus tissue supernatants of rats at 3, 24 h, 3, 7, and 14 days after the hypoxic exposure and their corresponding controls (C). Upper panel shows HIF-1α (120 kDa), VEGF (25 kDa), eNOS (140 kDa), iNOS (130 kDa), and nNOS (155 kDa) immunoreactive bands. Lower panel represents bar graphs (**A**, HIF-1α; **B**, VEGF; **C**, eNOS; **D**, iNOS; **E**, nNOS) showing significant changes in the optical density after hypoxic exposure.

Analysis of HIF-1α, VEGF, eNOS, iNOS, and nNOS protein expression by Western blotting (Figure 2)

The immunoreactive band of HIF-1α protein levels, approximately at 120 kDa, was increased significantly ($P < 0.05$) at 3 and 24 h after hypoxic exposure. Using VEGF antibody, an immunoreactive band of approximately 25 kDa was detected that was significantly increased ($P < 0.05$) at 3, 24 h, 3, and 7 days. At 14 days, it was declined below the control values. The densitometry of eNOS protein band was expressed approximately at 140 kDa and showed a significant increase at 3, 24 h, and 3 days after hypoxic exposure ($P < 0.05$), whereas at 7 and 14 days it was decreased significantly. The immunoreactive bands of iNOS and nNOS were expressed at 130 and 155 kDa respectively. The densitometry showed a significant increase ($P < 0.05$) up to 7 days for iNOS and 3 days for nNOS. In the latter, the protein expression was decreased at 7 and 14 days.

VEGF EIA (Figure 3A,C)

Analysis by EIA revealed that VEGF concentration increased significantly ($P < 0.05$) at 3 h to 7 days in hypoxic rats when compared with the controls. Thereafter, it declined but the reduction was not significant. VEGF concentration was suppressed significantly in rats given melatonin treatment.

Nitrite assay (Figure 3B,D)

The NO levels in the choroid plexus samples were significantly ($P < 0.05$) increased from 3 h to 7 days after hypoxia when compared with the controls. At 14 days, the difference between the control and hypoxic group was not significant. With melatonin administration, there was a significant decline in NO levels when compared with the hypoxic rats not given melatonin treatment.

Immunohistochemical analysis

Intraventricular and subependymal hemorrhages were consistent features in the hypoxic rats at various time points.

eNOS

eNOS expression was barely detected in the blood vessels in the choroid plexus in control rats (Figure 4A). Following hypoxic exposure at 3 and 24 h, many blood vessels exhibited enhanced eNOS immunoreactivity (Figure 4B). The eNOS immunoreactivity decreased at 3, 7, and 14 days after the exposure as compared with the earlier time intervals.

The eNOS expression was characterized by the wide occurrence of punctuate immunoreaction in the choroid plexus epithelial cells (Figure 4B). On closer examination, the reaction products were localized at the luminal surface of the epithelial cells (Figure 4B).

nNOS

Weak to moderate nNOS immunoexpression was observed in the choroid plexus epithelial cells in the control rats (Figure 4C). It was obviously augmented at 3, 24 h, and 3 days after the hypoxic exposure (Figure 4D), but was comparable to the controls in longer surviving rats.

iNOS

iNOS expression was absent in the choroid plexus in the control rats of all age groups (Figure 4E) but was markedly enhanced at 3 h following the hypoxic exposure (Figure 4F). At 24 h, 3, and 7 days, besides the choroid plexus epithelial cells, many intraventricular macrophages also showed intense iNOS expression (Figure 4F). At 14 days, iNOS expression was attenuated in both the choroid plexus epithelial cells and the intraventricular macrophages when compared with cells at earlier time intervals.

VEGF

VEGF expression was observed in the choroid plexus epithelial cells in the control rats at various time points (Figure 4G). Following the hypoxic exposure, the immunoexpression was increased up to 7 days (Figure 4H); thereafter, it was declined and was comparable to the controls.

CR3 receptors, MHC I, MHC II, and ED1 antigens

Intraventricular macrophages are selectively marked by monoclonal antibodies OX-42, OX-18, OX-6, and ED1 (32, 36) used in the present study. With OX-42, and at 3 h to 14 days after the hypoxic exposure, a large number of intraventricular macrophages expressing CR3 receptors were observed as compared with the corresponding controls (Figure 5A,B). Most of the cells in clusters were in close association with the choroid plexus (Figure 5B) and showed intense OX-42 immunoreactivity.

The results with ED1 paralleled that with OX-42, in which a large number of ED1 positive cells were observed at 3 h to 14 days after hypoxic exposure as compared with the controls (Figure 5C,D). With OX-18 and OX-6, very few immunoreactive cells were observed in the control rats in all groups (Figure 5E,G) but their numbers were markedly increased in the hypoxic rats at 24 h to 7 days (Figure 5F,H). In longer surviving rats, the immunoreactivity of intraventricular macrophages with OX-18 and OX-6 was comparable to cells in the control rats.

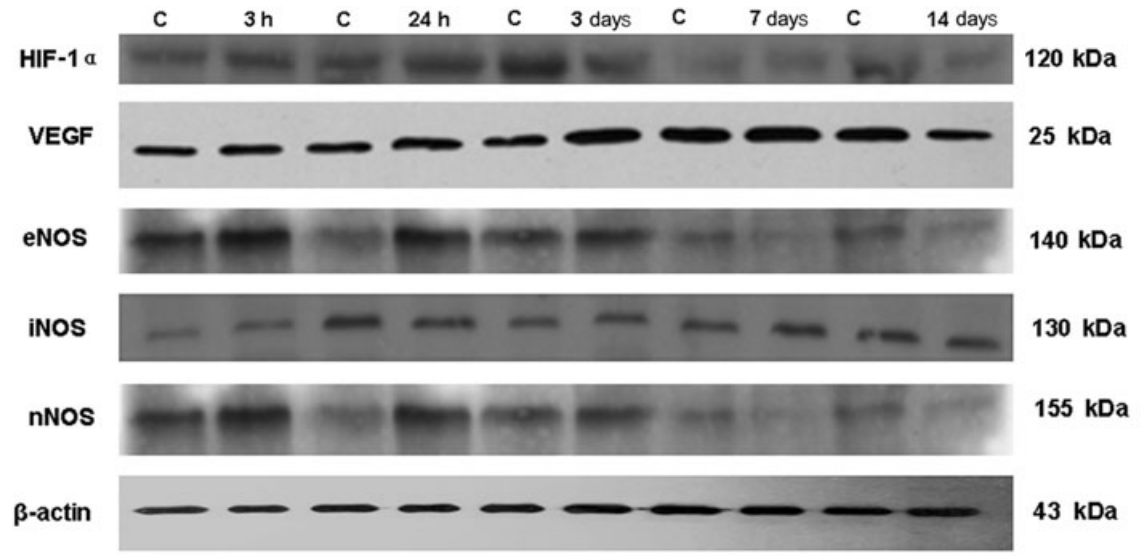

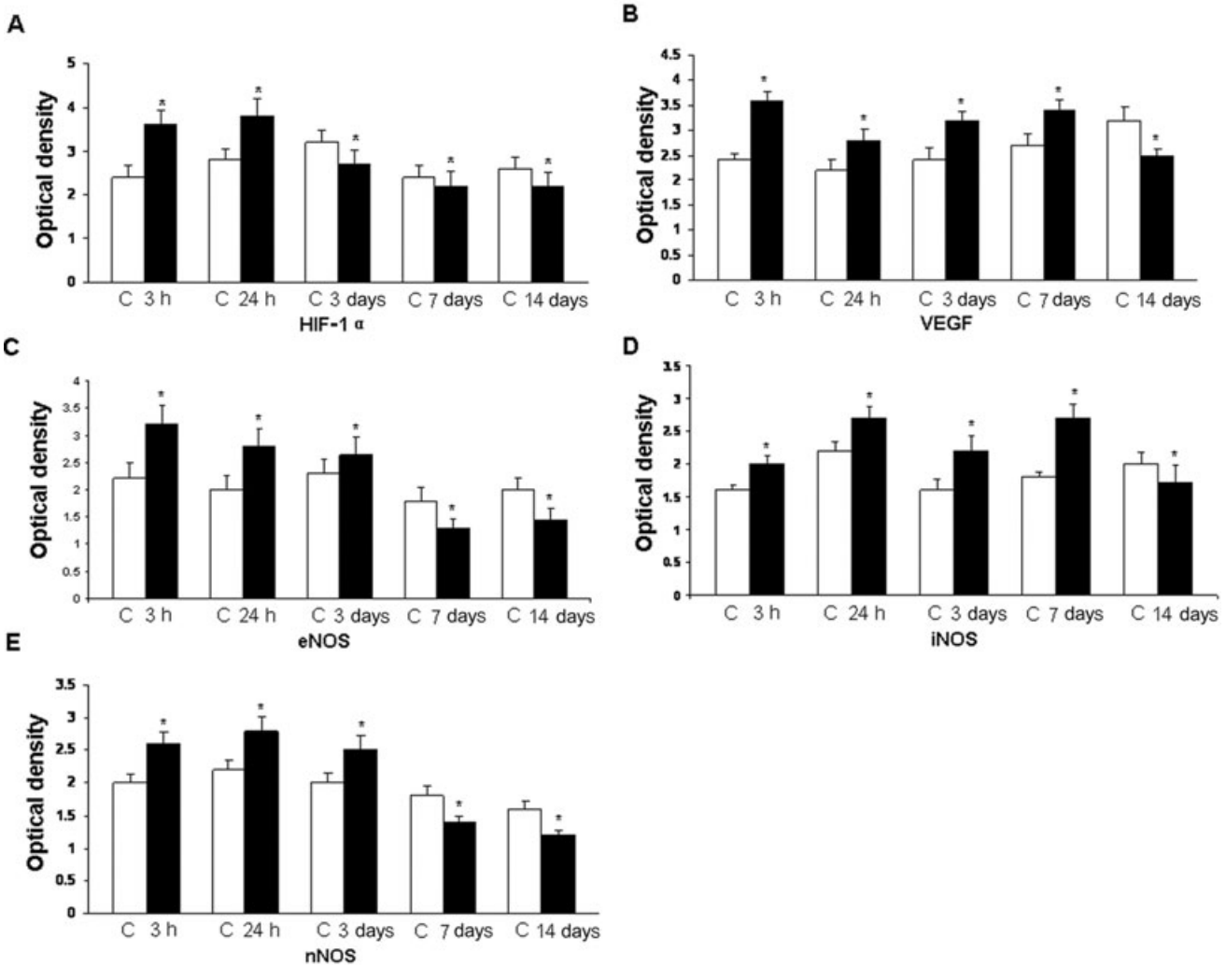

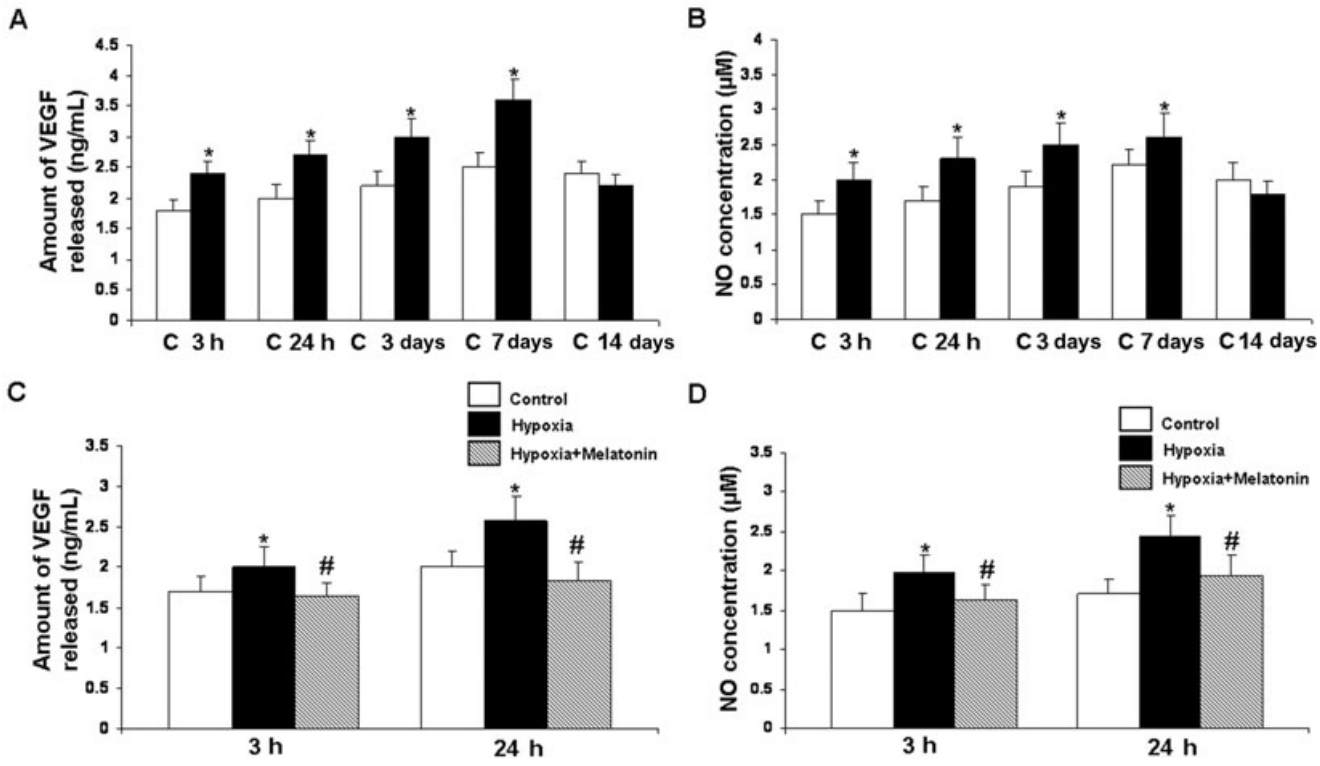

Figure 3. Vascular endothelial growth factor (VEGF) concentration (**A**) and nitric oxide (NO) production (**B**) in the postnatal rat choroid plexus of the control (**C**) and at 3, 24 h, 3, 7, and 14 days after hypoxia as determined by enzyme immunoassay and NO assay, respectively. Data represent mean ± SD. Significant differences between control and hypoxic rats are indicated by $*P < 0.05$. **C** and **D** show significant ($\#P < 0.05$) reduction in levels of VEGF and NO at 3 and 24 h in the choroid plexus after melatonin administration in hypoxic rats.

PAS staining

The choroid plexus epithelial cells in hypoxic rats showed intense PAS staining in the cytoplasm when compared with the corresponding controls (Figure 6).

Electron microscopy

Choroid plexus

In the control rats, the choroid plexus epithelial cells rested on a layer of basal lamina (Figure 7A) and their cytoplasm contained mitochondria, cisternae of rough endoplasmic reticulum, Golgi apparatus, and some electron dense bodies. Tight junctions were observed between the adjacent cells at the apical portions. Large numbers of tightly packed microvilli of uniform diameter projected into the ventricular lumen. Beginning at 3 h after the hypoxic exposure, the choroid plexus epithelial cells showed massive accumulation of glycogen in their cytoplasm (Figure 7B,C). Cytoplasmic vacuoles were observed in many epithelial cells at this stage. The intercellular spaces between the epithelial cells were widened but the tight junctions remained intact. At 24 h after the hypoxic exposure, the apical surface (the surface of the cell facing the ventricular lumen) of many epithelial cells showed eruption of cytoplasmic protrusions, either sessile or pedunculated, containing varying amounts of glycogen (Figure 7D). In some areas, detached profiles of these cytoplasmic fragments were observed to fill the ventricular lumen (Figure 7E).

At 3 days after the hypoxic exposure, the glycogen accumulation in the epithelial cells was reduced considerably. The cytoplasmic protrusions that occurred at earlier time intervals were less common. The intercellular spaces remained dilated and the tight junctions at the apical region were intact (Figure 7F). At 7 days, glycogen masses were absent. Furthermore, the cytoplasmic eruption was hardly seen at this stage. At 14 days, the epithelial cells showed features comparable to that in the control animals.

Intraventricular macrophages

In the control animals, occasional intraventricular macrophages either were closely associated with the microvilli of the epithelial cells or existed as free floating cells in the ventricle. The cells considered to be of the mononuclear phagocyte lineage (36) contained lysosomes, Golgi apparatus, cisternae of rough endoplasmic reticulum, and some vacuoles (Figure 7G). At 3 h to 7 days after the hypoxic exposure, they showed an accumulation of large cytoplasmic vacuoles and lysosomes (Figure 7H). Often they were surrounded by the cytoplasmic fragments that appeared to have been extruded into the ventricular lumen from the choroid plexus epithelial cells. At 7 days, the intraventricular macrophages remained

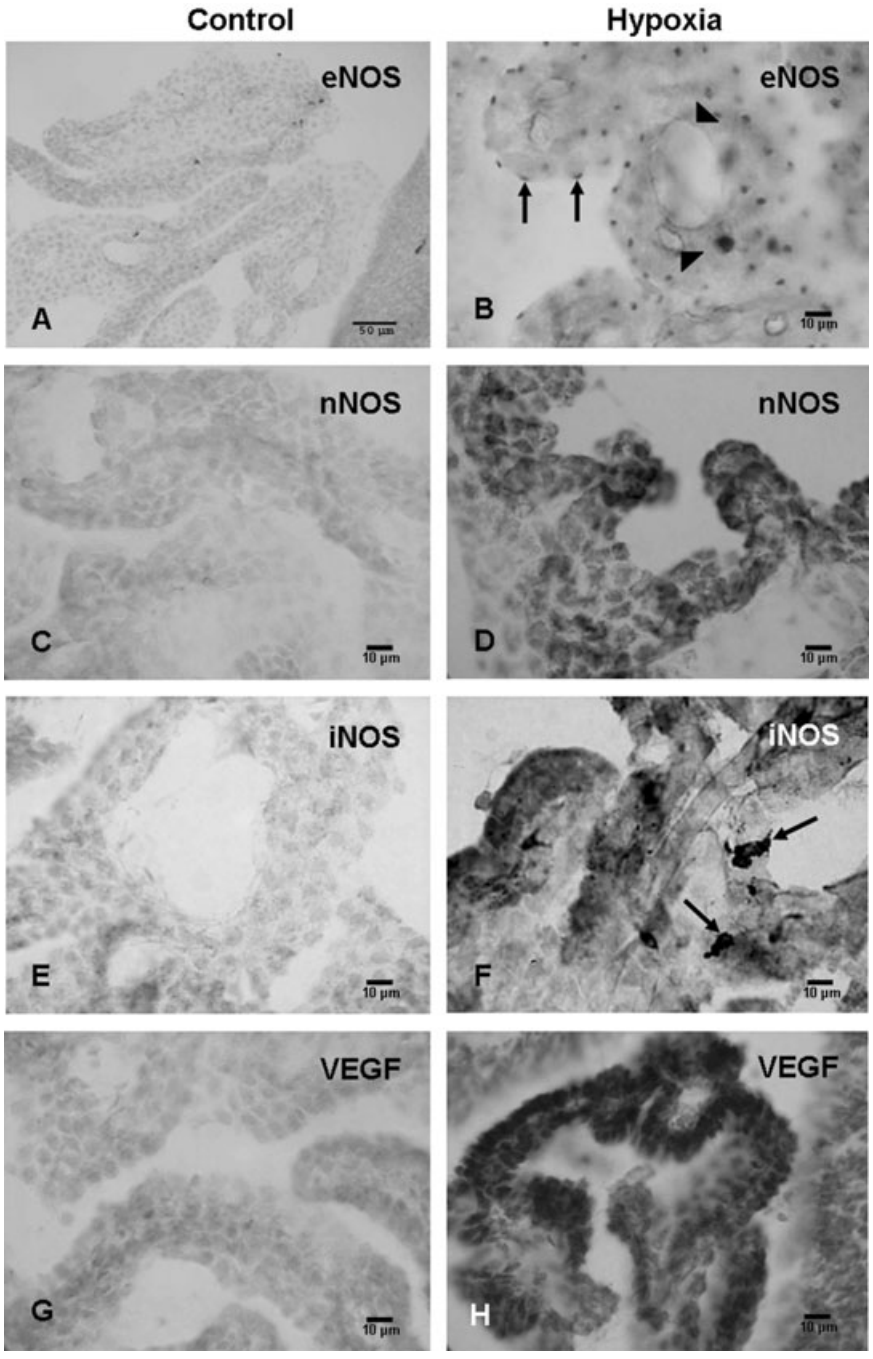

Figure 4. Endothelial nitric oxide synthase (eNOS) expression is detected in some blood vessels in the choroid plexus (CP) in a 1-day-old control rat (**A**) but not in the CP epithelial cells. Expression of eNOS is, however, enhanced at 3 h in the blood vessels (arrowheads) and the CP epithelial cells after the hypoxic exposure (**B**). The CP epithelial cells express eNOS immunoreactivity which is especially intense at their apical surfaces as focal dense spots (arrows, **B**). Weak neuronal nitric oxide synthase (nNOS) expression is detected in the choroid plexus in a 1-day-old control rat (**C**). It is noticeably enhanced at 24 h after the hypoxic exposure (**D**). Expression of inducible nitric oxide synthase (iNOS) is barely detected in the choroid plexus of a 1-day-old control rat (**E**). It is markedly induced at 24 h (**F**) in the epithelial cells of hypoxic rats. Many intraventricular macrophages (arrows) in hypoxic rats also exhibit intense iNOS expression in **F**. VEGF expression is greatly enhanced at 3 days (**H**) after the hypoxic exposure when compared with the corresponding controls (**G**).

laden with a large amount of lysosomes and vacuoles. By 14 days, these cells showed features comparable to those of the control animals.

Leakage of HRP

HRP reaction product was observed in the choroid plexus of the control rats at 3 h after an intravenous injection of the tracer (Figure 8A). Occasional intraventricular macrophages showed HRP labeling. In hypoxic rats, HRP reaction product was not localized in the choroid plexus. Instead, many intraventricular macrophages were filled with HRP reaction product (Figure 8B). In hypoxia + melatonin rats, HRP reaction product was seen to fill the intercellular spaces (Figure 8C). On the other hand, HRP-labeled intraventricular macrophages were absent.

DISCUSSION

Hypoxia/ischemia in the neonatal period is a major cause of brain damage. Cerebral palsy, epilepsy, motor, and visual disturbances

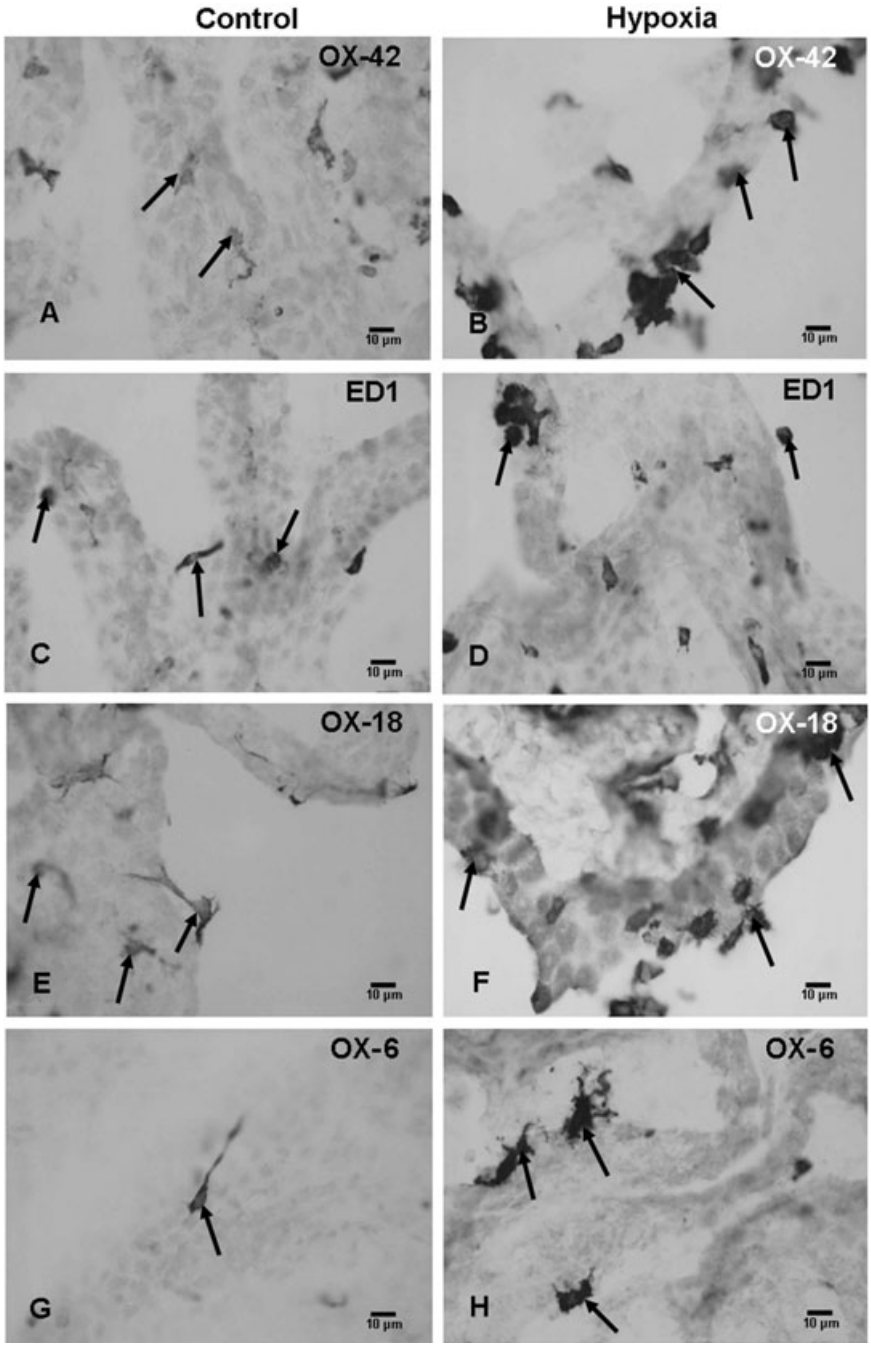

Figure 5. Few OX-42-positive intraventricular macrophages are associated with the choroid plexus in a 4-day-old control rat (**A**, arrows). At 3 days after exposure to hypoxia, a large number of OX-42-positive cells can be seen (**B**, arrows). Scattered ED1-positive cells (**C**, arrows) in a 4-day-old control rat as compared with a large number of ED1-positive cells at 3 days after the hypoxic exposure (**D**, arrows). OX-18-positive intraventricular macrophages in a 4-day-old control rat (**E**, arrows) and at 3 days after hypoxia (**F**, arrows). The numbers of OX-18-positive cells are drastically increased in the hypoxic rats. Many OX-6-positive cells can be seen at 3 days after hypoxic exposure (**H**, arrows) as compared with the corresponding controls in which occasional OX-6-positive epiplexus cells are identified (**G**, arrow).

have been reported to occur following such an insult (21). The periventricular white matter of the developing brain appears to be particularly vulnerable to damage following hypoxic/ischemic exposures (2, 17, 59), a condition being described as periventricular leukomalacia, perinatal telencephalic neuropathy, or subcortical leukoencephalopathy (15). Other complications of neonatal hypoxia such as intraventricular hemorrhage and ventricular dilatation (26, 43) have also been reported. Damage to the choroid plexus, ependyma, as well as the subependymal region has been described in hypoxic/ischemic conditions in the perinatal brain (50).

HIF-1α is expressed significantly in various tissues under hypoxic conditions and is known to activate the expression of many genes at the transcriptional level (52), VEGF being a bona fide target gene. Expression of VEGF persists for a longer time than that of HIF-1α (20, 49). This may be caused by decreased degradation of VEGF mRNA by hypoxia (11). VEGF is an angiogeneic mitogen whose actions are restricted to endothelial cells (5). It has been characterized as an inducer of vascular leakage (54) promoting the leakage of plasma proteins from blood vessels. The observation of VEGF expression in the epithelial cells of the choroid plexus in

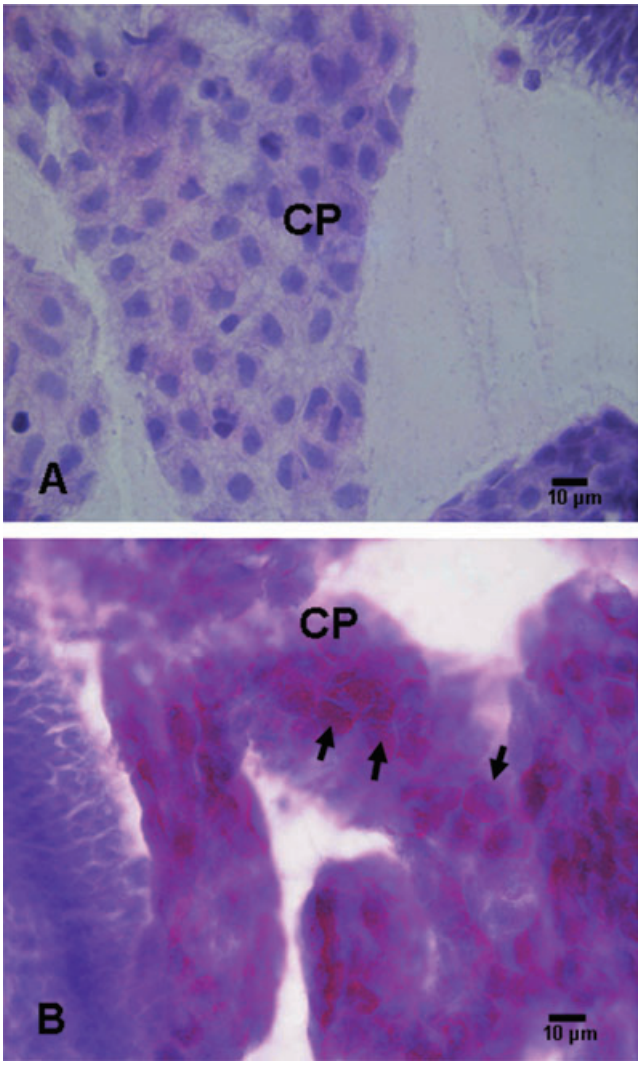

Figure 6. Periodic acid Schiff-stained choroid plexus (CP) epithelial cells in a 1-day-old control rat (**A**). Note the very light staining indicating a scarcity of glycogen accumulation in the cells. Intense PAS staining in **B** indicates a marked increase in glycogen accumulation in the CP epithelial cells (arrows) in hypoxic rats (**B**).

close contact to the fenestrated endothelium of blood vessels has led some investigators to speculate that VEGF may be involved in establishing or maintaining the fenestrated endothelium (5, 10). The fenestration of the endothelium reflects an increased permeability of the endothelial cells for low-molecular-weight substances (34). It has been reported that increased VEGF expression in adult mouse brains in hypoxic conditions leads to vascular leakage (51). The elevated VEGF mRNA and protein expression in hypoxic rats in the present study suggests increased vascular permeability in the choroid plexus. This is supported by rapid leakage of HRP in the ventricle and its uptake by intraventricular macrophages. Our earlier study (35) has shown that intravenously administered HRP diffuses to the CSF in postnatal rats. A large amount of the HRP was shown to accumulate in the intercellular spaces at 3 h after intravenous administration which was then endocytosed by the epithelial cells and released into the ventricular lumen to be picked up by the intraventricular macrophages (35) between 3 h and 6 h. In hypoxic rats in the present study, the intercellular spaces were clear of the HRP product at 3 h but the intraventricular macrophages showed intense labeling in comparison with the controls where only occasional cells were labeled suggesting that the passage of HRP into the ventricle was augmented.

VEGF has also been described as an inflammatory mediator that contributes to inflammatory responses observed in cerebral ischemia (7) in addition to its role in promoting increased vascular permeability. It may have a similar role in promoting inflammatory response in the hypoxic choroid plexus leading to tissue damage. Because of its pro-inflammatory actions, VEGF enhances the adhesion of leukocytes to vascular walls and increases intercellular cell adhesion molecule-1 and vascular cell adhesion molecule-1 expression (45).

Besides VEGF, there may be other factors contributing to increased vascular permeability. An earlier study (9) has shown increased levels of VEGF and NO in the CSF of newborn infants suffering from hypoxic ischemic encephalopathy. VEGF has been shown to induce increased vascular permeability via synthesis or release of NO (39) predominantly derived from eNOS (12). As vasodilatation and increase in blood flow occur in response to hypoxia, the enhanced expression of eNOS may also be involved in dilatation of blood vessels to increase the blood flow in hypoxic choroid plexus. NO, a potent vasodilator, has been implicated in the regulation of blood–brain barrier permeability (18). Leakage of serum-derived substances through the dilated blood vessels may lead to tissue damage in choroid plexus. Altered structural features of the choroid plexus epithelial cells were, in fact, observed in hypoxic rats. The eNOS expression at the apical surfaces of the epithelial cells may also be related to altered secretory activity of the choroid plexus epithelial cells. In relation to this, NO has been described to modulate the permeability of epithelial cells in the small intestine (29).

Along with eNOS, VEGF also induces expression of iNOS (27). Expansion of brain damage in ischemic conditions is known to occur through production of toxic levels of NO by iNOS (16). Expression of iNOS in the intraventricular macrophages and choroid plexus epithelial cells, as observed in the present study, may be responsible for producing the alterations in developing choroid plexus. *In vitro* studies have shown that NO produced by the microglial cells, considered as macrophages in the central nervous system, is highly damaging to the oligodendrocytes (44). Ohyu et al (47) carried out umbilical cord occlusion to evaluate fetal brain injury and reported that induction of iNOS in the activated microglia contributed to the tissue injury through NO overproduction. Excess NO production via iNOS has also been reported to contribute to increased permeability of the cerebral microvasculature in hypoxic injury (37). It is possible that NO derived from iNOS in the present study may also have a similar action on the blood vessels in the hypoxic choroid plexus.

Up-regulated mRNA and protein expression of nNOS after the hypoxic exposure is also a contributing factor to excess production of NO. It has been reported that both neuronal and epithelium-derived NO may regulate secretory function and hemodynamics of choroidal tissue (30). The secretory activity of the choroid plexus epithelial cells in the present study may have been altered as these cells were observed to extrude cytoplasmic fragments into the ven-

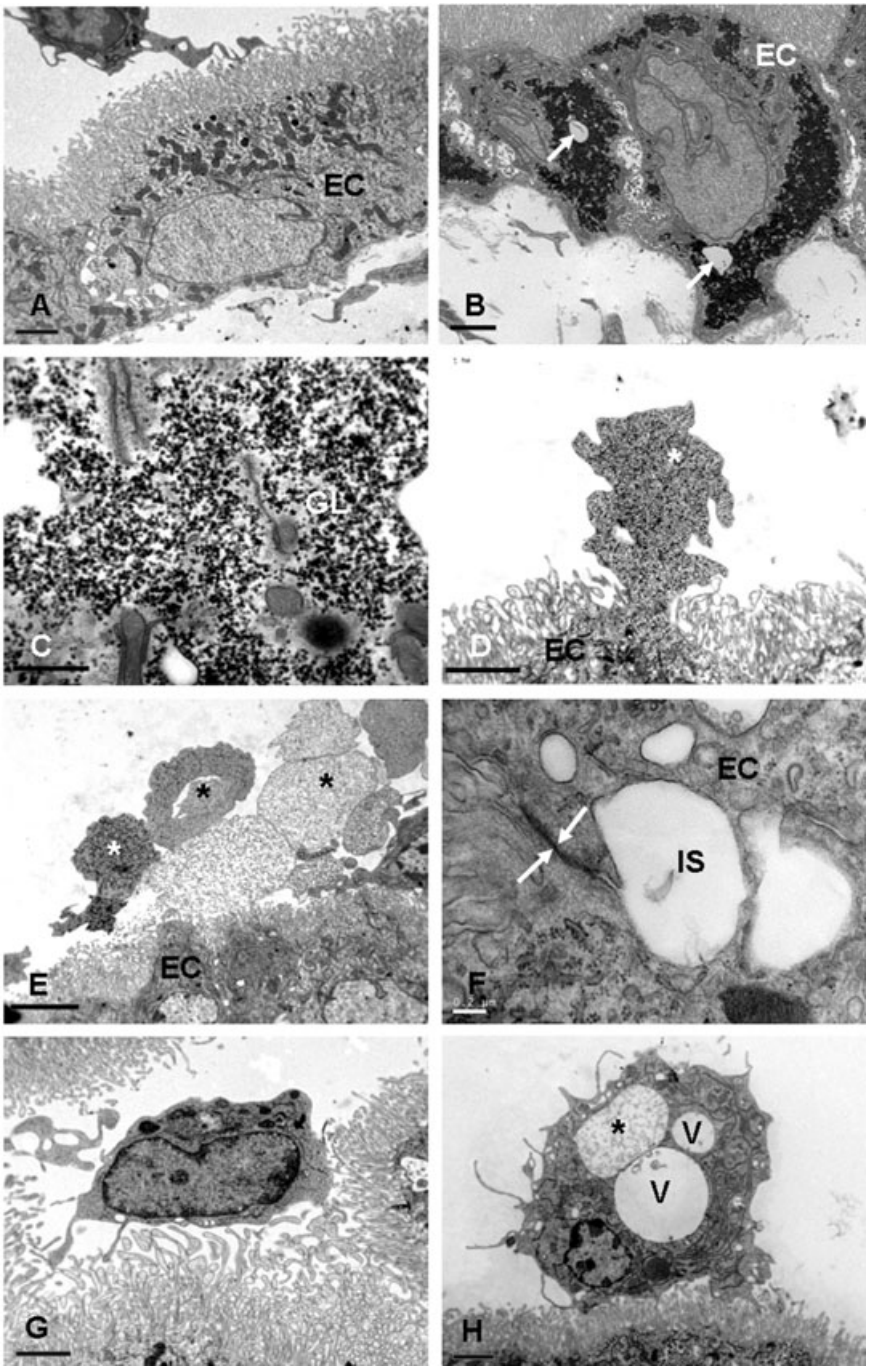

Figure 7. A. Choroid plexus of a control rat at 1 day of age. The epithelial cells (EC) show mitochondria, cisternae of rough endoplasmic reticulum, and some dense granules. The projecting microvilli are slender and uniform in diameter. **B.** Choroid plexus in a rat at 3 h after the hypoxic exposure. Note the massive accumulation of glycogen in the EC in **B**. Some cytoplasmic vacuoles (arrow) may be seen. **C** shows an enlarged view of glycogen (GL) accumulation in an epithelial cell at 3 h after hypoxic exposure. **D.** A choroid plexus EC at 24 h after the hypoxic exposure shows a sessile protrusion (asterisk) into the ventricular lumen. **E.** Many cytoplasmic fragments or profiles (asterisks) appear to be detached from the EC surfaces at 24 h after the hypoxic exposure. **F.** Intercellular spaces (IS) are widened between the EC at 3 days after hypoxic exposure. The tight junction (arrows) between the epithelial cells remains intact (**F**). **G.** An intraventricular macrophage in a 2-day-old control rat is in close association with the microvilli of the choroid plexus epithelial cells. **H.** An intraventricular macrophage at 24 h after the hypoxic exposure. Note the occurrence of large cytoplasmic vacuoles (V). One of them (asterisk) contains flocculent materials.

tricular lumen after the hypoxic exposure. This is supported by the rapid passage of HRP from circulation to the ventricular lumen in hypoxic rats.

The choroid plexus epithelial cells showed large accumulation of glycogen particles as well as cytoplasmic protrusions in the ventricular lumen at early time intervals following a hypoxic exposure. The microvilli in most of the epithelial cells in hypoxic rats were structurally similar to the microvilli observed in the control animals. Two types of microvilli have been described in relation to the secretory activity of the choroid epithelial cells, bulbous and filiform microvilli that are associated with increased and reduced CSF production, respectively (13). Although the microvilli appeared normal in the present study, the secretory activity of the choroid plexus appears to be altered because of the presence of numerous cytoplasmic extrusions from the apical surface of the epithelial cells. Extrusion of such cytoplasmic fragments from the choroid plexus epithelial cells was also observed in rats in our earlier study following the exposure of rats to a blast injury (23) and in cats (31) following a cisternal injection of crotoxin complex (Phospholipase A_2) indicating an altered CSF secretion. The cyto-

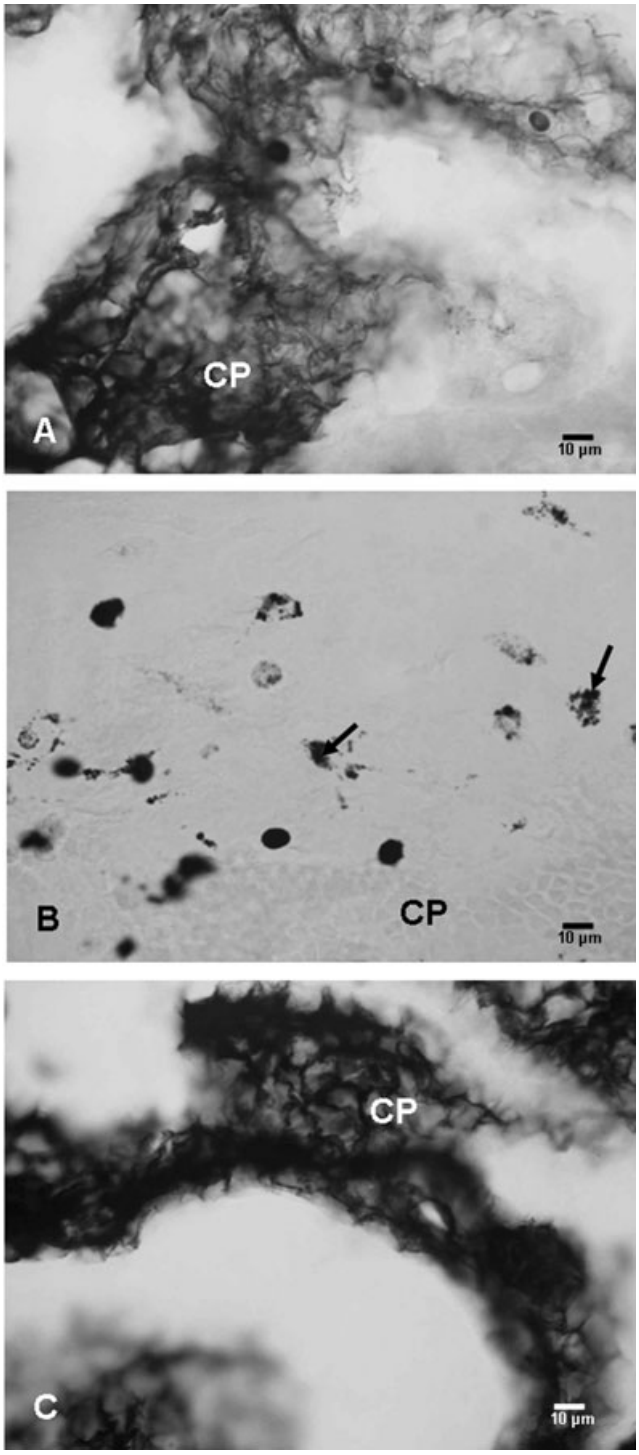

Figure 8. Choroid plexus (CP) in a control (**A**), hypoxic (**B**), and hypoxia + melatonin (**C**) administered rat showing horseradish peroxidase (HRP) reaction product. In **A** and **C**, massive accumulation of HRP reaction product is seen in the choroid plexus tissue in the epithelial cells and intercellular spaces, whereas in **B**, HRP accumulation is localized only in the intraventricular macrophages (arrows).

plasmic fragments were not observed in the ventricular lumen in longer surviving rats indicating that either they were engulfed by the numerous intraventricular macrophages or they were not being extruded by the epithelial cells.

The accumulation of large amounts of glycogen in the epithelial cells after the hypoxic exposure may be attributed to altered metabolic activity of the choroid plexus following a reduction in the oxygen supply. Cellular glycogen has been reported to be reduced in other cells such as myocytes during hypoxia (41), but was increased on restoration of normal oxygen tension (40, 55). In longer surviving rats, the above-mentioned changes had disappeared suggesting that with time the choroid plexus returned to normal. Structural restoration of the choroid plexus epithelium has been reported in the adult rats after transient forebrain ischemia (19).

The intraventricular macrophages also underwent structural alteration in the present study. They accumulated a large number of lysosomes and vacuoles which indicates an activation of the cell type. The up-regulation of CR3 receptors on these cells suggests an increase in their phagocytic function as they were frequently observed in the close vicinity of the cytoplasmic extrusions. The increased expression of MHC I and MHC II antigens following the hypoxic exposure suggests their involvement in an immunological response that may have been induced by the hypoxic environment. As intraventricular macrophages are known to originate from monocytes (32), increase in the number of ED1-positive cells suggests a rapid influx of these cells in the ventricular lumen in response to a greater demand for these cells to remove the cytoplasmic fragments being extruded by the epithelial cells.

Melatonin, a secretory product of the pineal gland, is known to decrease the NO levels in many tissues (1, 58) by inhibiting eNOS and iNOS production. It has also been shown to reduce nitrite/nitrate levels in serum of preterm infants with respiratory distress syndrome (14). The NO levels and VEGF tissue concentration in the choroid plexus declined following melatonin administration in the present study. This may be attributable to a decreased vascular leakage, and hence decreased leakage of HRP into the ventricular lumen and its subsequent uptake by intraventricular macrophages.

In conclusion, the present results suggest that a hypoxic exposure in the neonatal period elicits structural changes in the choroid plexus epithelial cells and possible alteration in the secretion of CSF. In response to these changes, the intraventricular macrophages showed an up-regulation of CR3 receptors, MHC I and MHC II and ED1 antigens. These features may be linked to increased receptor-mediated endocytosis and a possible immune response following the hypoxic exposure. The increased expression of VEGF, nNOS, eNOS, and iNOS point toward a key role of vascular permeability and NO in the development of hypoxic damage to the choroid plexus in neonatal period. This is supported by the observation that the ultrastructural changes observed in the choroid plexus correlated with the increase in NO production and VEGF concentration at these time points. Melatonin administration significantly suppressed VEGF concentration and NO production which conceivably had decreased the vascular leakage. Furthermore, it reduced the secretory activity of epithelial cells in hypoxic rats thus indicating its therapeutic potential in choroid plexus neuropathologies.

ACKNOWLEDGEMENTS

This study was supported by research grants (R181-000-065-112 and R181-000-098-112) from the National University of Singapore. The technical assistance of Mr P.C. Lim, Mr C.H. Yeo, Ms Y.G. Chan, and Mrs E.S. Yong is gratefully acknowledged.

REFERENCES

1. Alonso M, Collado PS, Gonzalez-Gallego J (2006) Melatonin inhibits the expression of the inducible isoform of nitric oxide synthase and nuclear factor kappa B activation in rat skeletal muscle. *J Pineal Res* **41**:8–14.
2. Banker BQ, Larroche JC (1962) Periventricular leukomalacia of infancy. A form of neonatal anoxic encephalopathy. *Arch Neurol* **7**:386–410.
3. Black SM, Bedolli MA, Martinez S, Bristow JD, Ferriero DM, Soifer SJ (1995) Expression of neuronal nitric oxide synthase corresponds to regions of selective vulnerability to hypoxia-ischaemia in the developing rat brain. *Neurobiol Dis* **2**:145–155.
4. Bolanos JP, Almeida A (1999) Roles of nitric oxide in brain hypoxia-ischemia. *Biochim Biophys Acta* **411**:415–436.
5. Breier G, Albrecht U, Sterrer S, Risau W (1992) Expression of vascular endothelial growth factor during embryonic angiogenesis and endothelial cell differentiation. *Development* **114**:521–532.
6. Cai Z, Hutchins JB, Rhodes PG (1998) Intrauterine hypoxia-ischemia alters nitric oxide synthase expression and activity in fetal and neonatal rat brains. *Brain Res Dev Brain Res* **109**:265–269.
7. Croll SD, Goodman JH, Scharfman HE (2004) Vascular endothelial growth factor (VEGF) in seizures: a double-edged sword. *Adv Exp Med Biol* **548**:57–68.
8. Emerich DF, Vasconcellos AV, Elliott RB, Skinner SJ, Borlongan CV (2004) The choroid plexus: function, pathology and therapeutic potential of its transplantation. *Expert Opin Biol Ther* **4**:1191–1201.
9. Ergenekon E, Gucuyener K, Erbas D, Aral S, Koc E, Atalay Y (2004) Cerebrospinal fluid and serum vascular endothelial growth factor and nitric oxide levels in newborns with hypoxic ischemic encephalopathy. *Brain Dev* **26**:283–286.
10. Esser S, Wolburg K, Wolburg H, Breier G, Kurzchalia T, Risau W (1998) Vascular endothelial growth factor induces endothelial fenestrations in vitro. *J Cell Biol* **140**:947–959.
11. Forsythe JA, Jiang BH, Iyer NV, Agani F, Leung SW, Koos RD, Semenza GL (1996) Activation of vascular endothelial growth factor gene transcription by hypoxia-inducible factor 1. *Mol Cell Biol* **16**:4604–4613.
12. Fukumura D, Gohongi T, Kadambi A, Izumi Y, Ang J, Yun CO, Buerk DG, Huang PL, Jain RK (2001) Predominant role of endothelial nitric oxide synthase in vascular endothelial growth factor-induced angiogenesis and vascular permeability. *Proc Natl Acad Sci USA* **98**:2604–2609.
13. Gabrion J, Maurel D, Clavel B, Davet J, Fareh J, Herbute S, O'Mara K, Gharib C, Hinds W, Krasnov I, Guell A (1996) Changes in apical organization of choroidal cells in rats adapted to spaceflight or head-down tilt. *Brain Res* **734**:301–315.
14. Gitto E, Romeo C, Reiter RJ, Impellizzeri P, Pesce S, Basile M, Antonuccio P, Trimarchi G, Gentile C, Barberi I, Zuccarello B (2004) Melatonin reduces oxidative stress in surgical neonates. *J Pediatr Surg* **39**:184–189.
15. Auer RN, Sutherland GR (2002) Hypoxia and related conditions. In: *Greenfiled's Neuropathology*. David I Graham and Peter L Lantos (eds), Chapter 5, pp. 233–280. Arnold: London.
16. Iadecola C, Zhang F, Casey R, Nagayama M, Ross ME (1997) Delayed reduction of ischemic brain injury and neurological deficits in mice lacking the inducible nitric oxide synthase gene. *J Neurosci* **17**:9157–9164.
17. Ikeda T, Choi H, Yee S, Murata Y, Quilligan EJ (1999) Oxidative stress, brain white matter damage and intrauterine asphyxia in fetal lambs. *Int J Dev Neurosci* **17**:1–14.
18. Janigro D, West GA, Nguyen TS, Winn HR (1994) Regulation of blood-brain barrier endothelial cells by nitric oxide. *Circ Res* **75**:528–538.
19. Johanson E, Palm DE, Primiano MJ, McMillan PN, Chan P, Knuckey NW, Stopa EG (2000) Choroid plexus recovery after transient forebrain ischemia: role of growth factors and other repair mechanisms. *Cell Mol Neurobiol* **20**:197–216.
20. Josko J, Mazurek M (2004) Transcription factors having impact on vascular endothelial growth factor (VEGF) gene expression in angiogenesis. *Med Sci Monit* **10**:RA89–RA98.
21. Kadhim H, Evrard PH, Kahn A, DE Prez C, Bonnier CH, Sebire G (2005) Insights into Etiopathogenic Mechanisms Involved in Perinatal Cerebral Injury: Implications for Neuroprotection. In: *Focus on Cerebral Palsy Research*. HD Fong (ed.), pp. 1–26. Nova Science Pub Inc, New York.
22. Kadhim H, Khalifa M, Deltenre P, Casimir G, Sebire G (2006) Molecular mechanisms of cell death in periventricular leukomalacia. *Neurology* **67**:293–299.
23. Kaur C, Singh J, Lim MK, Ng BL, Yap EP, Ling EA (1996) Studies of the choroid plexus and its associated epiplexus cells in the lateral ventricles of rats following an exposure to a single non-penetrative blast. *Arch Histol Cytol* **59**:239–248.
24. Kaur C, Sivakumar V, Zhang Y, Ling EA (2006) Hypoxia-induced astrocytic reaction and increased vascular permeability in the rat cerebellum. *Glia* **4**:826–839.
25. Kaur C, Sivakumar V, Lu J, Ling EA (2007) Increased vascular permeability and nitric oxide production in response to hypoxia in the pineal gland. *J Pineal Res* **42**:338–349.
26. Kirks DR, Bowie JD (1986) Cranial ultrasonography of neonatal periventricular/intraventricular hemorrhage: who, how, why and when? *Pediatr Radiol* **16**:114–119.
27. Kroll J, Waltenberger J (1998) VEGF-A induces expression of eNOS and iNOS in endothelial cells via VEGF receptor-2 (KDR). *Biochem Biophys Res Commun* **252**:743–746.
28. Kuban K, Sanocka U, Leviton A, Allred EN, Pagano M, Dammann O, Share J, Rosenfeld D, Abiri M, DiSalvo D, Doubilet P, Kairam R, Kazam E, Kirpekar M, Schonfeld S (1999) White matter disorders of prematurity: association with intraventricular hemorrhage and ventriculomegaly. The Developmental Epidemiology Network. *J Pediatr* **134**:539–546.
29. Kubes P (1992) Nitric oxide modulates epithelial permeability in the feline small intestine. *Am J Appl Pathol* **262**:G1138–G1142.
30. Lin AY, Szmydynger-Chodobska J, Rahman MP, Mayer B, Monfils PR, Johanson CE, Lim YP, Corsetti S, Chodobski A (1996) Immunohistochemical localization of nitric oxide synthase in rat anterior choroidal artery, stromal blood microvessels, and choroid plexus epithelial cells. *Cell Tissue Res* **285**:411–418.
31. Ling EA, Gopalakrishnakone P, Tan CK (1988) Electron-microscopical study of the choroid plexus and epiplexus cells in cats following a cisternal injection of crotoxin complex. *Acta Anat* **131**:241–248.
32. Ling EA, Kaur C, Lu J (1998) Origin, nature, and some functional considerations of intraventricular macrophages, with special reference to the epiplexus cells. *Microsc Res Tech* **41**:43–56.
33. Livak KJ, Schmittgen TD (2001) Analysis of relative gene expression data using real-time quantitative PCR and the 2(-Delta Delta C (T)) method. *Methods* **24**:402–408.
34. Levick JR, Smaje LH (1987) An analysis of the permeability of a fenestra. *Microvasc Res* **33**:233–256.

35. Lu J, Kaur C, Ling EA (1993) Uptake of tracer by the epiplexus cells via the choroid plexus epithelium following an intravenous or intraperitoneal injection of horseradish peroxidase in rats. *J Anat* **183**:609–617.
36. Lu J, Kaur C, Ling EA (1994) Up-regulation of surface antigens on epiplexus cells in postnatal rats following intraperitoneal injections of lipopolysaccharide. *Neuroscience* **63**:1169–1178.
37. Mark KS, Burroughs AR, Brown RC, Huber JD, Davis TP (2004) Nitric oxide mediates hypoxia-induced changes in paracellular permeability of cerebral microvasculature. *Am J Physiol Heart Circ Physiol* **286**:H174–H180.
38. Mashayekhi F, Draper CE, Bannister CM, Pourghasem M, Owen-Lynch PJ, Miyan JA (2002) Deficient cortical development in the hydrocephalic Texas (H-Tx) rat: a role for CSF. *Brain* **125**:1859–1874.
39. Mayhan WG (1999) VEGF increases permeability of the blood-brain barrier via a nitric oxide synthase/cGMP-dependent pathway. *Am J Physiol* **276**:C1148–C1153.
40. McNulty PH, Luba MC (1995) Transient ischemia induces regional myocardial glycogen synthase activation and glycogen synthesis in vivo. *Am J Physiol* **268**:H364–H370.
41. McNulty PH, Ng C, Liu WX, Jagasia D, Letsou GV, Baldwin JC, Soufer R (1996) Autoregulation of myocardial glycogen concentration during intermittent hypoxia. *Am J Physiol* **271**:R311–R319.
42. Melillo G, Musso T, Sica A, Taylor LS, Cox GW, Varesio L (1995) A hypoxia-responsive element mediates a novel pathway of activation of the inducible nitric oxide synthase promoter. *J Exp Med* **182**:1683–1693.
43. Ment LR, Schwartz M, Makuch RW, Stewart WB (1998) Association of chronic sublethal hypoxia with ventriculomegaly in the developing rat brain. *Brain Res Dev Brain Res* **111**:197–203.
44. Merrill JE, Ignarro LJ, Sherman MP, Melinek J, Lane TE (1993) Microglial cell cytotoxicity of oligodendrocytes is mediated through nitric oxide. *J Immunol* **151**:2132–2141.
45. Min JK, Lee YM, Kim JH, Kim YM, Kim SW, Lee SY, Gho YS, Oh GT, Kwon YG (2005) Hepatocyte growth factor suppresses vascular endothelial growth factor-induced expression of endothelial ICAM-1 and VCAM-1 by inhibiting the nuclear factor-kappaB pathway. *Circ Res* **96**:300–307.
46. Miyan JA, Nabiyouni M, Zendah M (2003) Development of the brain: a vital role for cerebrospinal fluid. *Can J Physiol Pharmacol* **81**:317–328.
47. Ohyu J, Marumo G, Ozawa H, Takashima S, Nakajima K, Kohsaka S, Hamai Y, Machida Y, Kobayashi K, Ryo E (1999) Early axonal and glial pathology in fetal sheep brains with leukomalacia induced by repeated umbilical cord occlusion. *Brain Dev* **21**:248–252.
48. Orihara Y, Ikematsu K, Tsuda R, Nakasono I (2001) Induction of nitric oxide synthase by traumatic brain injury. *Forensic Sci Int* **123**:142–149.
49. Ozaki H, Yu AY, Della N, Ozaki K, Luna JD, Yamada H, Hackett SF, Okamoto N, Zack DJ, Semenza GL, Campochiaro PA (1999) Hypoxia inducible factor-1alpha is increased in ischemic retina: temporal and spatial correlation with VEGF expression. *Invest Opthalmol Vis Sci* **40**:182–189.
50. Rothstein RP, Levison SW (2002) Damage to the choroid plexus, ependyma and subependyma as a consequence of perinatal hypoxia/ischemia. *Dev Neurosci* **24**:426–436.
51. Schoch HJ, Fischer S, Marti HH (2002) Hypoxia-induced vascular endothelial growth factor expression causes vascular leakage in the brain. *Brain* **125**:2549–2557.
52. Semenza GL (1998) Hypoxia-inducible factor 1: master regulator of O2 homeostasis. *Curr Opin Genet Dev* **8**:588–594.
53. Semenza GL (2000) HIF-1: using two hands to flip the angiogenic switch. *Cancer Meatastasis Rev* **19**:59–65.
54. Senger DR, Galli SJ, Dvorak AM, Perruzzi CA, Harvey VS, Dvorak HF (1983) Tumor cells secrete a vascular permeability factor that promotes accumulation of ascites fluid. *Science* **219**:983–985.
55. Silverman HS, Wei S, HaigneyMC, Ocampo CJ, Stern MD (1997) Myocyte adaptation to chronic hypoxia and development of tolerance to subsequent acute severe hypoxia. *Circ Res* **80**:699–707.
56. Stopa EG, Berzin TM, Kim S, Song P, Kuo-LeBlanc V, Rodriguez-Wolf M, Baird A, Johanson CE (2002) Human choroid plexus growth factors: what are the implications for CSF dynamics in Alzheimer's disease? *Exp Neurol* **167**:40–47.
57. Szmydynger-Chodobska J, Monfils PR, Lin AY, Rahman MP, Johanson CE, Chodobski A (1996) NADPH-diaphorase histochemistry of rat choroid plexus blood vessels and epithelium. *Neurosci Lett* **208**:179–182.
58. Tamura EK, Silva CL, Markus RP (2006) Melatonin inhibits endothelial nitric oxide production in vitro. *J Pineal Res* **41**:267–274.
59. Volpe JJ (2001) *Neurology of the Newborn*. WB Saunders: Philadelphia.
60. Weller RO (1998) Pathology of cerebrospinal fluid and interstitial fluid of the CNS: significance for Alzheimer disease, prion disorders and multiple scleroses. *J Neuropathol Exp Neurol* **57**:885–894.
61. Xue M, Balasubramaniam J, Buist RJ, Peeling J, Del Bigio MR (2003) Periventricular/intraventricular hemorrhage in neonatal mouse cerebrum. *J Neuropathol Exp Neurol* **62**:1154–1165.
62. Young PP, Fantz CR, Sands MS (2004) VEGF disrupts the neonatal blood–brain barrier and increases life span after non-ablative BMT in a murine model of congenital neurodegeneration caused by a lysosomal enzyme deficiency. *Exp Neurol* **188**:104–114.